Pergamon

*Int. J. Heat Mass Transfer.* Vol. 39, No. 4, pp. 801–809, 1996

0017-9310/96 $15.00 + 0.00

0017-9310(95)00151-4

# Friction pressure drop of R-12 in small hydraulic diameter extruded aluminum tubes with and without micro-fins

C-Y. YANG and R. L. WEBB†

Department of Mechanical Engineering, The Pennsylvania State University, University Park, PA 16802, U.S.A.

(*Received* 17 *August* 1994 *and in final form* 5 *April* 1995)

**Abstract**—Adiabatic, single-phase liquid and two-phase flow pressure drop were measured for R-12 flowing in both rectangular plain and micro-fin tubes with hydraulic diameters 2.64 and 1.56 mm, respectively. The single-phase liquid friction factors for the plain and micro-fin tubes are uniformly 14% and 36% higher, respectively, than that predicted by the Blasius equation. For two-phase flow, the pressure gradient increases with increasing mass velocity and vapor quality. The pressure gradient of the micro-fin tube is higher than that of the plain tube at same mass velocity and vapor quality. Predictive methods for the single-phase liquid and two-phase friction factor were also developed. These data are not well correlated by the Chisholm correlation which uses the Lockhart–Martinelli two-phase multiplier. However, the equivalent mass velocity concept proposed by Akers *et al.* provided a very good correlation of the present data. Both the plain and micro-fin tube data are correlated within ±20% by a single curve.

This work shows that the pressure drop is dominated by vapor shear in both the plain and micro-fin tubes. Vapor shear effects in micro-fin tube do not cause significant disturbances in the two-phase flow. This observation provides additional evidence to support the conclusion in other work by Yang and Webb that the distinctly steep condensation heat transfer curves at low mass velocity and high vapor quality are caused by surface tension drainage force.

## INTRODUCTION

In Yang and Webb [1], condensation heat transfer coefficients were reported for R-12 flow in horizontal, flat, extruded aluminum plain and micro-fin tubes. The hydraulic diameter range encompassed 1.56–2.64 mm. Based on evaluation of their data, they propose that both vapor shear and surface tension forces can influence the condensing coefficient. Surface tension effects are greatest for low mass velocity and vapor qualities greater than 0.5. This paper reports the pressure drop data on the same tubes studied by Yang and Webb [1]. A correlation to predict the single-phase and two-phase pressure drop as a function of fluid properties is also developed.

Wambsganss *et al.* [2] and [3] measured the pressure drop for single and two-phase air-water flow in plain rectangular channels having dimensions 19.05 × 3.18 mm and 9.52 × 1.59 mm ($D_h$ = 5.45 and 2.72 mm). They found that the single-phase friction factor can be predicted very well by the Blasius friction factor equation based on hydraulic diameter. However, their two-phase data plotted in the form of the two-phase multiplier vs the Martinelli parameter did not correlate well. Damianides [4] measured air-water two-phase flow pressure drop in round tubes with i.d. of 1, 2, 3, 4 and 5 mm and compared his data with the Lockhart–Martinelli correlation. He reported wide scatter, with errors up to 100%.

Pressure drop data for refrigerant condensation and evaporation in circular plain and micro-fin tubes (4–15 mm diameter) have been extensively reported (e.g. Thors and Bogart [5] and Chamra *et al.* [6]). However, none of the investigators of the round micro-fin tube have sought to develop correlations for prediction of the single or two-phase pressure drop as a function of internal geometry and fluid properties. An important element of this work is development of predictive methods for the single-phase and two-phase friction factor in both rectangular plain and micro-fin tubes.

## TEST FACILITIES

Figure 1 shows photographs of tube tested, and Fig. 2 shows a schematic diagram of the test facility. Details of the test facility and tube dimensions were described by Yang and Webb [1]. The internal port dimensions of the two tubes are identical, except tube (b) has 0.2 mm high micro-fins, at 0.4 mm lateral pitch. The cross-sectional flow areas of the two tubes were obtained from enlarged cross-section photographs of the tube samples actually tested. The profiles of the 20× photos were scanned using AutoCAD software to determine the cross-sectional area of each

† Author to whom correspondence should be addressed.

## NOMENCLATURE

| | |
|---|---|
| $A$ | total heat transfer surface area [m$^2$] |
| $A_c$ | cross-sectional flow area [m$^2$] |
| $A_i$ | inside tube surface area [m$^2$] |
| $A_o$ | outside tube surface area [m$^2$] |
| $b$ | tube minor outside diameter [m] |
| $c_p$ | specific heat [J kg$^{-1}$] |
| $D$ | diameter [m] |
| $D_h$ | hydraulic diameter of flow passages, $4LA_c/A$ [m] |
| $e$ | fin height [m] |
| $G$ | mass velocity in tube, $G_v$ (of vapor component), $G_l$ (of liquid component) [kg m$^{-2}$ s$^{-1}$] |
| $G_{eq}$ | equivalent mass velocity, $G[(1-x)+x(\rho_l/\rho_v)^{1/2}]$ [kg m$^{-2}$ s$^{-1}$] |
| $h$ | heat transfer coefficient. $h_l$ (liquid phase flowing alone), $h_m$ (micro-fin tube), $h_p$ (plain tube), $h$ (average) [W m$^{-2}$ K$^{-1}$] |
| $h_{fg}$ | latent heat [kJ kg$^{-1}$] |
| $k$ | thermal conductivity [W m$^{-1}$ K$^{-1}$] |
| $L$ | flow length [m] |
| $m$ | mass flow rate [kg s$^{-1}$] |
| $Nu$ | Nusselt number, $hD/k_l$ |
| $p$ | fluid pressure [Pa] |
| $p_{cr}$ | critical pressure [Pa] |
| $P$ | wetted perimeter [m] |
| $Pr$ | Prandtl number |
| $q''$ | heat flux [W m$^{-2}$] |
| $Q$ | heat transfer rate [W] |
| $r$ | local radius [m] |
| $Re_{D_h}$ | Reynolds number ($GD_h/\mu_l$) |
| $Re_{eq}$ | equivalent Reynolds number ($G_{eq}D_h/\mu_l$) |
| $Re_L$ | Reynolds number for two-phase flow based on total mass rate flowing as liquid ($G_LD_h/\mu_l$) |
| $s$ | coordinate distance along curved condensing profile [m] |
| $t$ | tube wall and internal membrane thickness [m] |
| $T$ | temperature. $T_w$ (water), $T_{sat}$ (saturation) [°C] |
| $U$ | overall heat transfer coefficient [W m$^{-2}$ K$^{-1}$] |
| $w$ | tube outside major diameter [m] |
| $x$ | vapor quality (average in tube). |

Greek symbols

| | |
|---|---|
| $\Gamma$ | condensate mass velocity [kg m$^{-1}$ s$^{-1}$] |
| $\delta$ | condensate film thickness [m] |
| $\Delta T_{ln}$ | log-mean temperature difference [°C] |
| $\Delta x$ | vapor quality change |
| $\mu$ | dynamic viscosity $\mu_l$ (of liquid), $\mu_v$ (of vapor) [kg m$^{-1}$ s$^{-1}$] |
| $\sigma$ | surface tension [N m$^{-2}$]. |

Subscripts

| | |
|---|---|
| i | designates inner surface of tube |
| l | liquid phase |
| L | total mass rate flowing as liquid |
| m | micro-fin tube |
| o | designates outer surface of tube |
| p | plain tube |
| r | refrigerant |
| t | test section |
| v | vapor phase |
| w | water. |

flow channel. These cross-sectional areas are 27.27 and 22.68 mm$^2$ for tubes (a) and (b), respectively.

Figure 3 shows the inlet–exit plenum used for the differential pressure measurement taps. Pressure drop data were measured inside a 560 mm long, horizontal tube under adiabatic conditions for all-liquid, and for two-phase flow. The data spanned $2500 < Re_{D_h} < 23\,000$ for single-phase liquid flow, and $400 < G < 1400$ kg m$^{-2}$ s$^{-1}$ and vapor qualities of $0.1 < x < 0.9$ for two-phase flow. The pressure drop was measured by a differential pressure transducer accurate within $\pm 0.2\%$ of the calibrated span (110 kPa).

## DATA REDUCTION

Because no heat transfer occurred in the horizontal test section, no acceleration and gravity terms are included in the measured pressure drop. The measured pressure drop ($\Delta P_{exp}$) includes the friction ($\Delta p_f$), entrance ($\Delta p_i$) and exit ($\Delta p_e$) pressure drop components defined by

$$\Delta p_{exp} = \Delta p_f + \Delta p_i - \Delta p_e. \quad (1)$$

For single-phase liquid flow $\Delta p_i$ and $\Delta p_e$ can be calculated by the equations:

$$\Delta p_i = \frac{G^2}{2\rho_l}(1-\sigma^2+K_c) \quad (2)$$

$$\Delta p_e = \frac{G^2}{2\rho_l}(1-\sigma^2-K_e) \quad (3)$$

where $\sigma$ is the ratio of the test section cross-sectional area to the frontal area of the inlet and exit plenums, $A_c/A_{fr}$. The $K_c$ and $K_e$ are functions of $\sigma$ and Reynolds number. Kays and London [7] provide graphs to determine $\sigma$ for several cross sectional shapes. We used their Fig. 5-4, which is for a square cross-section.

Collier and Thome [8] recommend use of a sep-

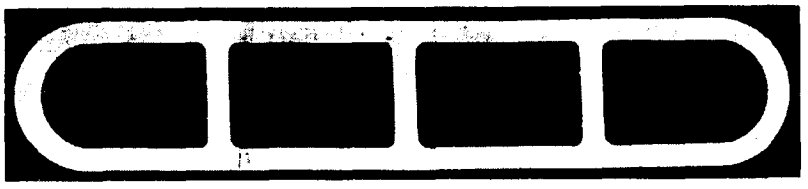

(a) Plain tube

(b) Micro-fin tube

Fig. 1. Photographs of tube tested.

arated flow model for calculation of $\Delta p_i$ and $\Delta p_e$ in two-phase flow. Their recommended equations for a sudden expansion and a sudden contraction are given by equations (4) and (5), respectively.

$$\Delta p_e = G^2\sigma(1-\sigma)v_l\left[\frac{(1-x)^2}{(1-\alpha)}+\left(\frac{v_v}{v_l}\right)\frac{x^2}{\alpha}\right] \quad (4)$$

$$\Delta p_i = \left(\frac{G}{C_c}\right)^2(1-C_c)\left[\frac{(1+C_c)\left(\frac{x^3v_v^2}{\alpha^2}+\frac{(1-x)^3v_l^2}{(1-\alpha)^2}\right)}{2[xv_v+(1-x)v_l]}\right.$$

$$\left.-C_c\left(\frac{x^2v_v}{\alpha}+\frac{(1-x)^2v_l}{(1-\alpha)}\right)\right] \quad (5)$$

where $\alpha$ is the void fraction which can be calculated from Zivi [9] equation

$$\alpha = \left[1+\frac{1-x}{x}\left(\frac{\rho_v}{\rho_l}\right)^{2/3}\right]^{-1}. \quad (6)$$

Note that sudden contraction equation [equation (5)] contains the "coefficient of contraction," ($C_c$), rather than the contraction ratio ($\sigma$). The term $C_c$ is defined as $A_{vc}/A_c$, where $A_{vc}$ is the flow area of the vena contracta for single-phase flow. Collier and Thome [8] give numerical values of $C_c$ as a function of $\sigma$ for turbulent, single-phase flow.

Table 1 shows the ratio of friction pressure drop to measured pressure drop. Table 1 shows that typically $0.82 < \Delta p_f/\Delta p_{exp} < 0.97$. Hence, uncertainties associated with evaluation of the entrance and exit losses are quite small.

The friction factor is defined in terms of the hydraulic diameter. For single-phase liquid flow, it is defined as:

$$f_l = \frac{\Delta p_f}{G^2/2\rho_l}\frac{D_h}{4L} = \frac{\Delta p_f}{Re_{D_h}^2\mu_l^2/2\rho_l}\frac{D_h^3}{4L} \quad (7)$$

where $L$ is the tube length.

For two-phase flow, the friction factor is defined in terms of an equivalent all-liquid flow that will give the same frictional pressure drop as the two-phase flow. This two-phase friction factor is defined as:

$$f = \frac{\Delta p_f}{G_{eq}^2/2\rho_l}\frac{D_h}{4L} = \frac{\Delta p_f}{Re_{eq}^2\mu_l^2/2\rho_l}\frac{D_h^3}{4L} \quad (8)$$

where $G_{eq}$ is the equivalent liquid mass velocity proposed by Akers *et al.* [10] and is given by:

$$G_{eq} = G\left[(1-x)+x\left(\frac{\rho_l}{\rho_v}\right)^{1/2}\right]. \quad (9)$$

The equivalent all-liquid Reynolds number is defined as:

$$Re_{eq} = \frac{G_{eq}D_h}{\mu_l}. \quad (10)$$

Table 1. Ratio of friction pressure drop to measured pressure drop

| $\Delta P_f/\Delta P_{exp}$ | Micro-fin tube | Plain tube |
|---|---|---|
| Liquid | | |
| $G = 400$ | 0.93 | 0.86 |
| $G = 1400$ | 0.91 | 0.82 |
| Two-phase | | |
| $G = 400$ | 0.96 ($x = 0.17$) | 0.95 ($x = 0.12$) |
| | 0.93 ($x = 0.90$) | 0.84 ($x = 0.90$) |
| $G = 1400$ | 0.97 ($x = 0.12$) | 0.94 ($x = 0.11$) |
| | 0.93 ($x = 0.51$) | 0.88 ($x = 0.41$) |

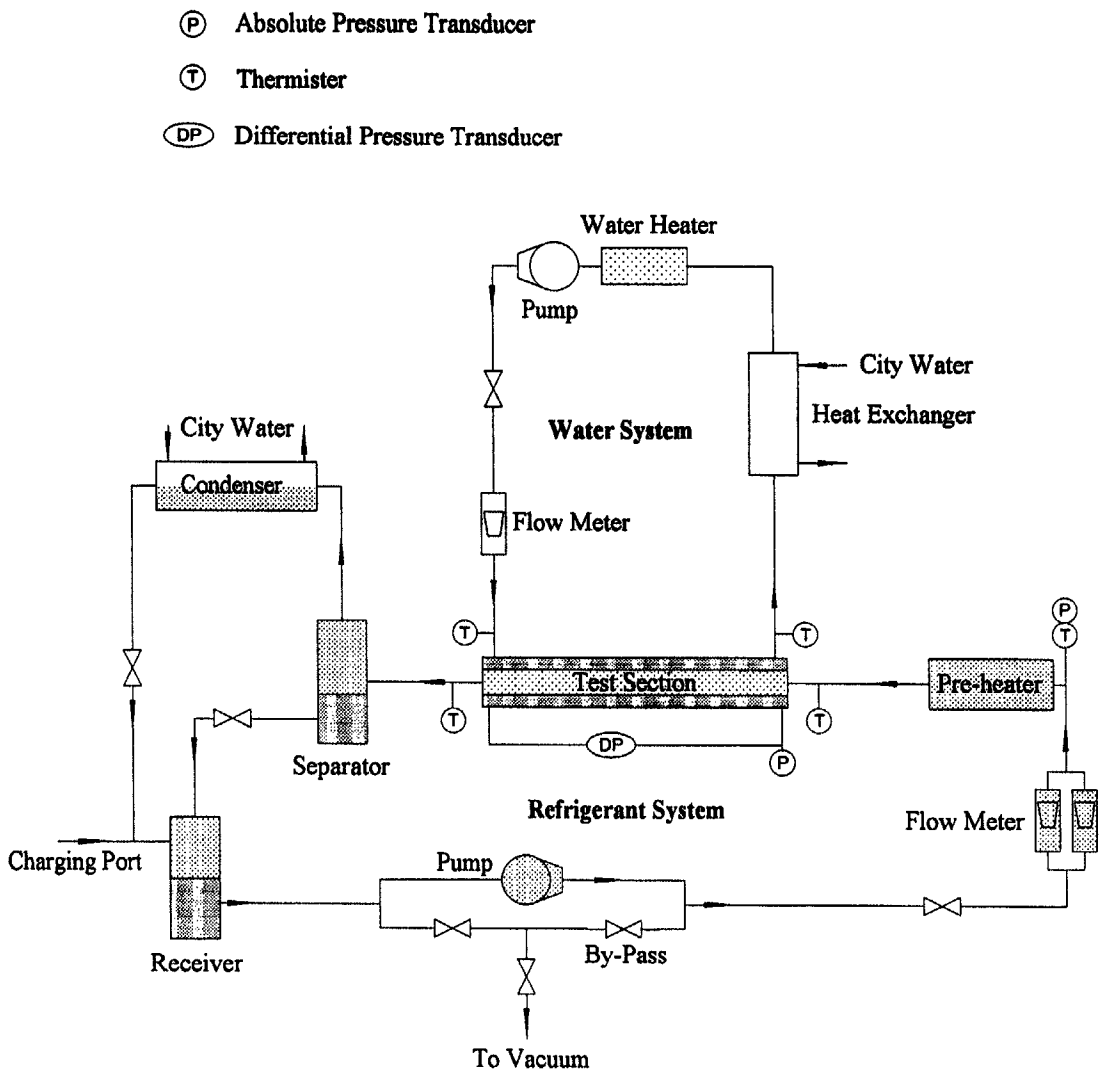


Fig. 2. Schematic diagram of test facility.

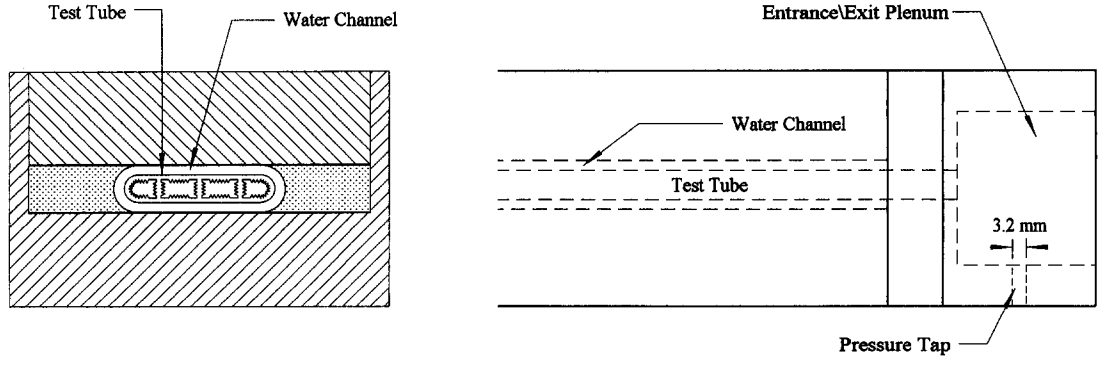


Fig. 3. Measurement of pressure drop.

## EXPERIMENTAL RESULTS

*Subcooled liquid flow pressure drop*

Figure 4(a) shows the frictional pressure drop ($\Delta p_f$) vs mass velocity ($G$) and Fig. 4(b) shows $\Delta p_f$ plotted vs $Re_{D_h}$ ( $= GD_h/\mu_l$). As expected, the pressure drop increases with increasing mass velocity, or with increasing $Re_{D_h}$. For the same mass velocity, the pressure drop in the micro-fin tube is approximately two times that in the plain tube. The friction factor ($f_l$), defined by equation (7), is shown in Fig. 5 vs $Re_{D_h}$. Figure 5 also shows $f_l$ vs $Re_{D_h}$ for fully developed, turbulent flow in smooth channels. The solid line shows the smooth tube, Blasius friction factor equation ($0.079\ Re^{-0.25}$) based on hydraulic diameter. The lowest experimental $Re_{D_h} \cong 2500$. The friction factors for the plain and micro-fin tubes are uniformly 14% and 36% higher, respectively, than that predicted by Blasius equation. The curve fitted equations for the tested plain and micro-fin tubes are shown in Fig. 5.

It is of interest to compare the single-phase friction and Nusselt number characteristics of the micro-fin tube. The hydraulic diameter based Nusselt number for micro-fin tube, as reported by Yang and Webb [1], is smaller than that for plain tube. Figure 5 shows that the friction factor of the micro-fin tube is larger than that of the plain tube. Hence, the ratio of $(Nu_m/Nu_p)/(f_m/f_p)$ is less than one. This result is consistent with the measurements of Carnavos [11] for single phase flow in internally finned tubes having axial and helical fins as stated by Webb [12].

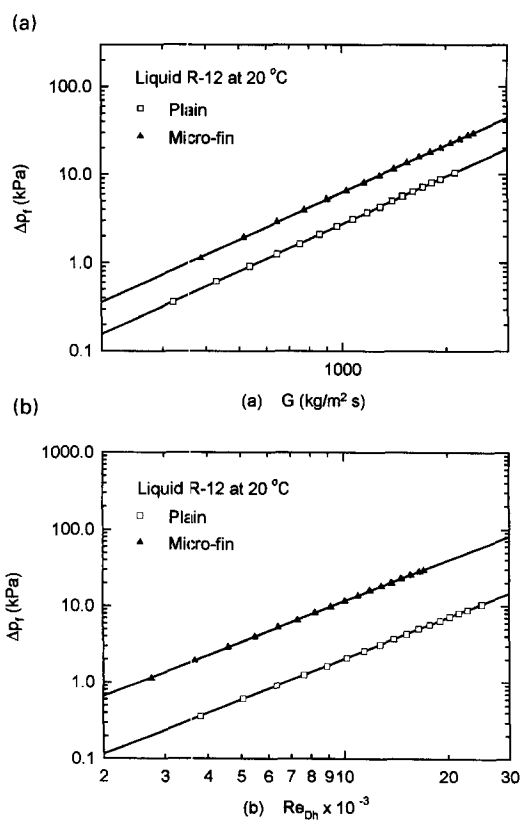


Fig. 4. Single-phase liquid flow pressure drop in plain and micro-fin tubes; (a) $\Delta p_f$ vs $G$, (b) $\Delta p_f$ vs $Re_{D_h}$.

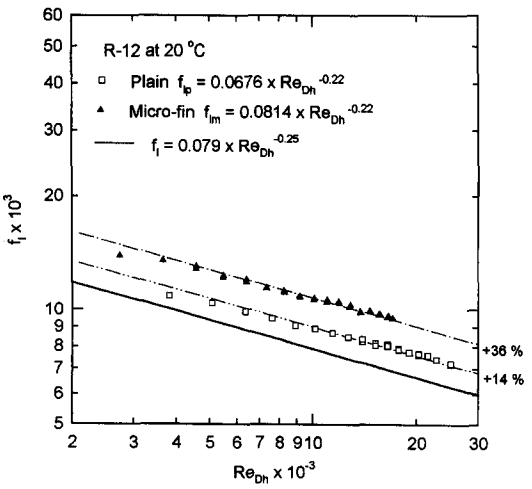


Fig. 5. Single-phase liquid friction factor in plain and micro-fin tubes; plain tube: $f_{lp} = 0.0676 \times Re_{D_h}^{-0.22}$; micro-fin tube: $f_{lm} = 0.0814 \times Re_{D_h}^{-0.22}$.

*Two-phase flow pressure drop*

Figure 6 shows the two-phase flow friction pressure gradient inside a plain tube plotted vs vapor quality for mass velocities of $G = 400$, 600, 1000 and 1400 kg $m^{-2}$ $s^{-1}$. The micro-fin frictional pressure gradient data are shown in Fig. 7 for the same range of flow conditions. Both figures show that the pressure drop increases with increasing mass velocity and vapor quality. The pressure drop of the micro-fin tube is higher than that of the plain tube at same mass velocity and vapor quality. For example, at $G = 1000$ kg $m^{-2}$ $s^{-1}$ and $x = 0.5$, the micro-fin pressure drop is 2.2 times that of the plain tube.

## PRESSURE DROP CORRELATION

Work has been done to correlate the two-phase frictional pressure drop data for the plain and micro-

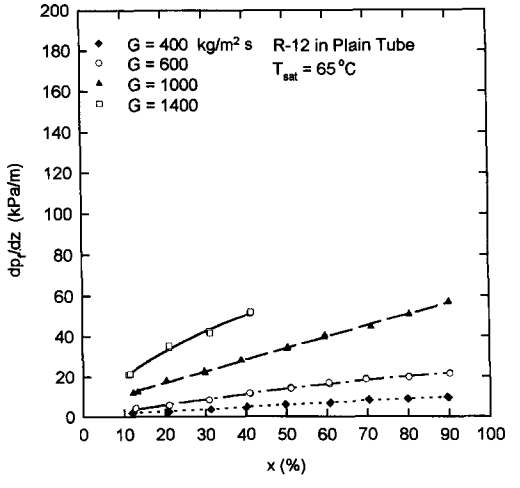


Fig. 6. Two-phase flow pressure drop in a plain tube.

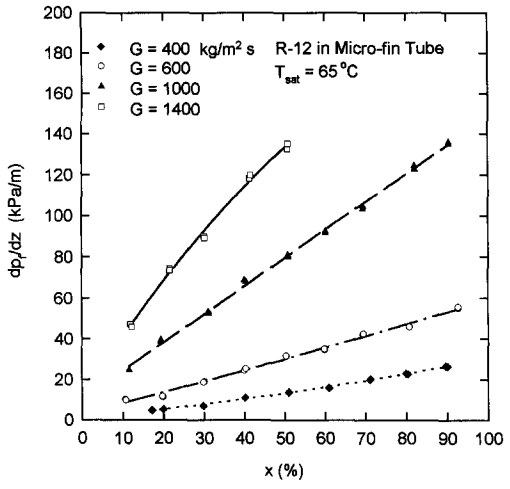


Fig. 7. Two-phase flow pressure drop in a micro-fin tube.

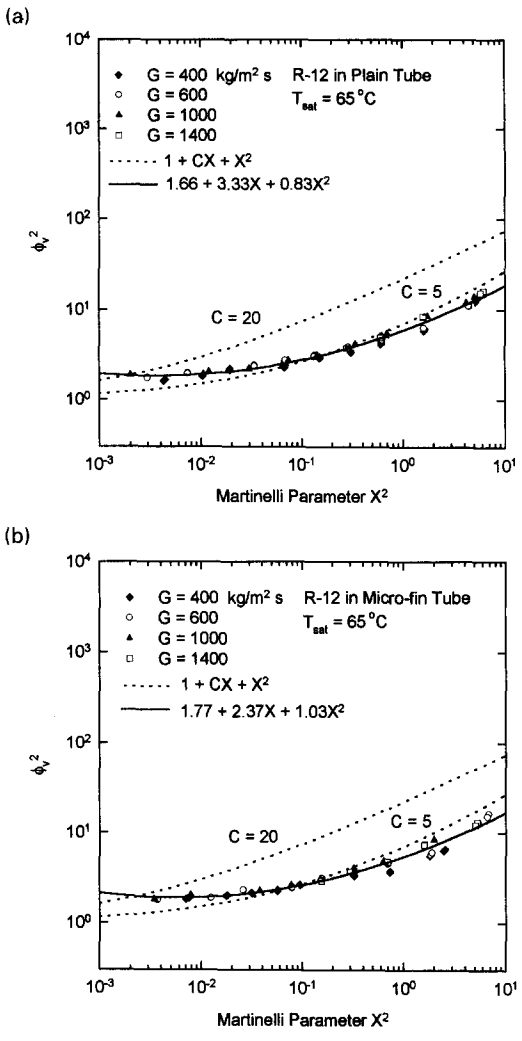


Fig. 8. Two-phase multiplier vs Martinelli parameter in terms of different mass velocity; (a) plain tube, (b) micro-fin tube.

fin tubes. Two methods have been evaluated. These are described below.

*Lockhart and Martinelli method*

Lockhart and Martinelli [13] proposed a semi-empirical separated flow model, which is described by Collier and Thome [8]. For plain, circular tubes, Collier and Thome [8] show that one may correlate the friction data in the form $\phi_l^2 = fcn(X)$, where $\phi_l^2$ is the two-phase multiplier which is defined as $\phi_l^2 = (dp_f/dz)/(dp_{f,l}/dz)$ and $X^2$ is the Martinelli parameter, which is calculated for the liquid and vapor phases flowing alone in the tube, $(dp_{f,l}/dz)/(dp_{f,v}/dz)$. Alternately, one may correlate the data in the form $\phi_v^2 = (dp_f/dz)/(dp_{f,v}/dz)$. They show that the correlation is given by either of the following two equivalent forms proposed by Chisholm [14]:

$$\phi_l^2 = 1 + \frac{C}{X} + \frac{1}{X^2} \tag{11a}$$

$$\phi_v^2 = 1 + CX + X^2. \tag{11b}$$

The constant $C$ ranges from 5 to 20, depending on whether the liquid and vapor phases are laminar or turbulent. We have chosen to use the form of equation (11b), because the term $f_v$ is within the turbulent range for the range of data shown on Figs. 6 and 7.

Figures 8(a) and (b) show the measured data plotted in the form $\phi_v^2$ vs $X^2$ and that predicted by equation (11b) for $C = 5$ and 20. This calculation is sensitive to whether each phase is laminar or turbulent. The friction factor used for calculation of $(dp_{f,v}/dz)$ for each geometry is taken from Fig. 5. According to Chisholm [14], $C = 20$ is applicable if the vapor and liquid phases flowing alone are both turbulent. Or, if both phases flowing alone are laminar, $C = 5$. Figure 8 shows that equation (11b) will not correlate the data (e.g. there is no single constant $C$ applicable to equation (11b) which will correlate the data). Also shown in Figs. 8(a) and (b) are our empirical correlations for the $\phi_v^2$ vs $X^2$ data.

Figure 9 shows the actual conditions existing for each data point, where the legend symbols are having the following interpretation: vv (viscous liquid/viscous vapor), tv (turbulent liquid/viscous vapor), vt (viscous liquid/turbulent vapor) and tt (turbulent liquid/turbulent vapor). Figures 9(a) and (b) show that only the "vt" and "tt" conditions exist for the present data. Thus, the vapor phase flowing alone is always turbulent ($Re_v > 2000$). Examination of the figure shows that the data corresponding to $C = 20$ would be very poorly predicted by equation (11b). For example, at $X^2 = 1$, the ratio of the predicted and experimental values of $(dp_f/dz) \cong 3.5$. The present results are consistent with those of Wambsganss *et al.* [15], who also showed that the Lockhart and Martinelli method does a poor job of correlating their air–water data in small hydraulic diameter, rectangular channels. Use of the empirical correlation of $\phi_v^2$ vs $X^2$

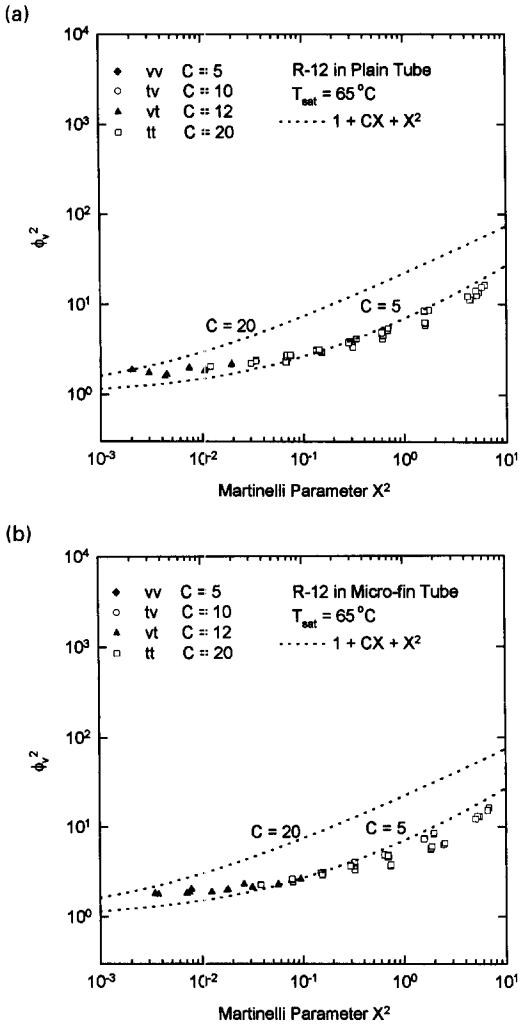


Fig. 9. Two-phase multiplier vs Martinelli parameter in terms of different flow regime: (a) plain tube; (b) micro-fin tube.

shown in Fig. 8(a) and (b) will provide a reasonably good prediction of the data.

Martinelli and Nelson [16] assumed that the Lockhart–Martinelli correlation is correct at atmospheric pressure. They surmised that the two-phase multiplier may decrease with increasing reduced pressure, and that $\phi_v^2$ approaches unity as the system pressure nears the critical point. They developed a graphical form of their correlation for steam, which accounts for the effect of reduced pressure. The reduced pressure at the present test condition is approximately 0.4. The Martinelli and Nelson's graphical correlation predicts a value of $\phi_v^2$ that is within 30% of our experimental data.

*Akers* et al. *method*

An alternate approach to correlating the friction data is that proposed by Akers *et al.* [10]. This friction factor is defined by equation (8) and is that for an equivalent all-liquid flow at an equivalent all-liquid Reynolds number defined by equation (10).

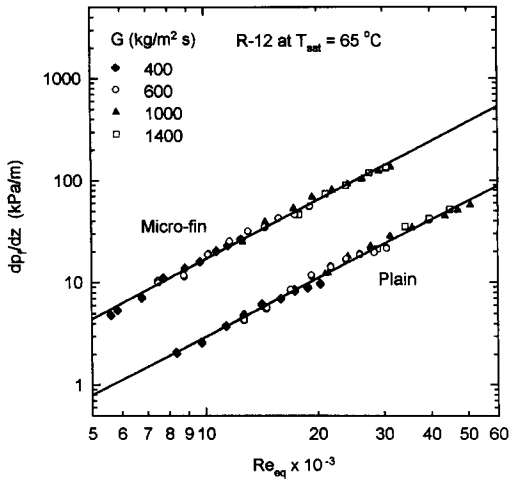


Fig. 10. Comparison of two-phase flow pressure gradient in plain and micro-fin tubes based on equivalent Reynolds number.

Figure 10 shows the measured pressure gradient vs the equivalent Reynolds number. Figure 11 combines the single-phase liquid and two-phase flow pressure gradient plotted vs the equivalent Reynolds number, $Re_{eq}$. These figures show very good correlation of the data, especially single-phase liquid and two-phase flow at high mass velocity and high vapor quality, for each tube geometry.

Figure 12 shows the two-phase friction factor defined by equation (8) plotted vs $Re_{eq}$ for both the plain and micro-fin tubes. The figure shows a very small dependence of the friction factor on Reynolds number, $f \propto (Re_{eq})^{-0.1}$. Figure 13 shows the ratio of the two-phase and single-phase friction factors plotted vs $Re_{eq}$. The $f_l$ is the single-phase friction factor for the liquid phase flowing alone. Both the plain and micro-fin tube data are correlated within $\pm 20\%$ by a

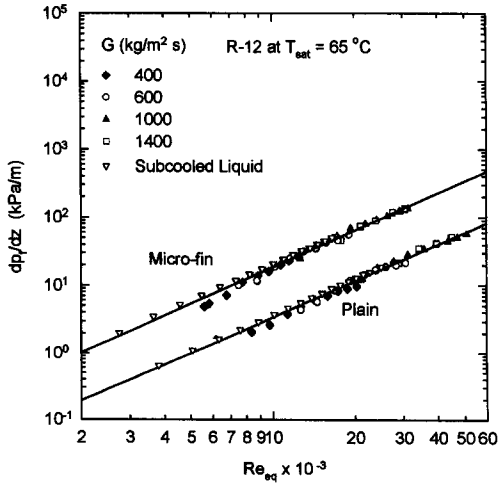


Fig. 11. Combined single-phase liquid and two-phase pressure gradient in plain and micro-fin tubes.

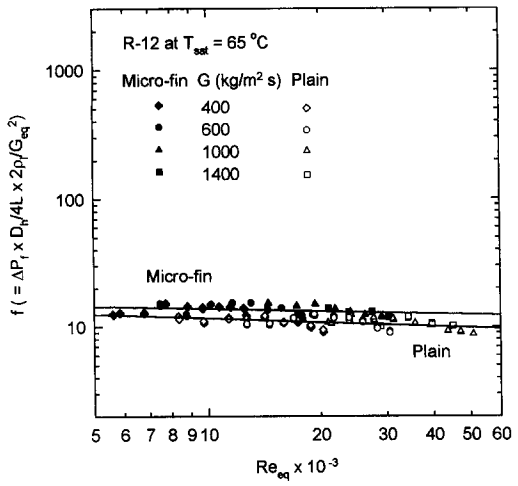


Fig. 12. Two-phase friction factor for flow in plain and micro-fin tubes.

single curve. The equation of the correlation shown in Fig. 13 is given by

$$\frac{f}{f_l} = 0.435 Re_{eq}^{0.12}. \quad (12)$$

The correlation given by equation (12) accounts for fluid properties, so it should be applicable to different fluids. The geometry dependence is included via the $f_l$ term. Because $f_l$ is not independent of geometry (Fig. 5), one must obtain single-phase friction data for the geometry of interest.

To calculate the two-phase pressure drop at specified $G$ and $x$ using equation (12), one performs the following steps:

(1) Calculate $Re_{D_h}$ for the liquid phase flowing alone. Then calculate the single-phase friction factor from the correlation given in Fig. 5. Based on the data range shown in Fig. 5, the correlation is applicable for $Re_{D_h}$ in the turbulent range (e.g. $Re_{D_h} > 2500$).

(2) Calculate $Re_{eq}$ for the two-phase flow using equation (10).

(3) Calculate $f$ using equation (12).

(4) Calculate the two-phase friction pressure gradient using equation (8).

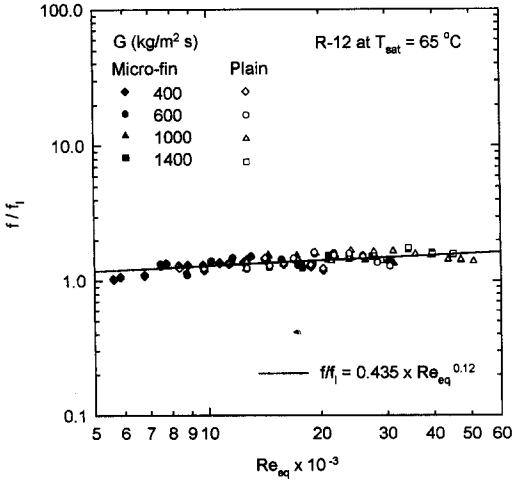


Fig. 13. Ratio of the two-phase and single-phase liquid friction factors.

## DISCUSSION

The tubes tested in the present study are so small that manufacturing tolerance on the tube wall thickness can have a significant effect on the calculated friction factor. The tube manufacturer states that the tolerance on the wall thickness is $\pm 0.05$ mm. The maximum tolerance would cause a 5% error in the cross-section area ($A_c$). Because $f \propto A_c^3$, a 5% error in $A_c$ would result in 15.7% uncertainty of the friction factor (for fixed flow rate). Our cross-sectional areas are based on careful measurements of the tube samples actually tested.

Yang and Webb [1] measured the R-12 condensation coefficient using the same tubes tested here. They concluded that surface tension force exerts a significant effect on the condensation coefficient at low mass velocity and high vapor quality (above 0.5). They speculated that the condensate film was so thin that surface tension force contributed to drainage of the film from the tips of the micro-fins. Hence, for the low mass velocity and higher vapor quality conditions, both vapor shear and surface tension forces act to thin the condensate film. It is of value to determine if surface tension force also affects the frictional pressure drop.

For single-phase flow, equation (7) shows that $\Delta p_{f,l} \propto f_l (Re_{D_h})^2$. Similarly, for two-phase flow, equation (8) shows that $\Delta p_f \propto f (Re_{eq})^2$. Hence, for $Re_{D_h} = Re_{eq}$

$$\frac{\Delta p_f}{\Delta p_{f,l}} = \frac{f}{f_l}. \quad (13)$$

Figure 13 shows the ratios $f_m/f_{lm}$ and $f_p/f_{lp}$ for the micro-fin and plain tubes, respectively. Figure 13 shows that both $f_m/f_{lm}$ and $f_p/f_{lp}$ are well correlated by a single curve, for all mass velocities and vapor qualities tested. Because vapor shear is the only force which contributes to the frictional pressure drop in the plain tube, we conclude that it is the only significant force operative in the micro-fin tube. Surface tension force plays no significant role in affecting the frictional pressure drop in the micro-fin tube.

## CONCLUSIONS

The single-phase liquid friction factors for the plain and micro-fin tubes are uniformly 14% and 36% higher, respectively, than that predicted by Blasius equation.

For two-phase flow, the pressure gradient increases

with increasing mass velocity and vapor quality. The pressure gradient in the micro-fin tube is higher than that of the plain tube at same mass velocity and vapor quality.

These data are not well correlated by the Lockhart–Martinelli two-phase multiplier. However, the equivalent mass velocity concept proposed by Akers *et al.* [10] provided a very good correlation of the present data. Both the plain and micro-fin tube data are correlated within $\pm 20\%$ by a single curve.

It appears that surface tension force plays no significant role in affecting the frictional pressure drop in the micro-fin tube.

*Acknowledgement*—The extruded aluminum tubes tested were provided by Showa Aluminum Co. We are also grateful for the financial support of Showa Aluminum Co.

## REFERENCES

1. C-Y. Yang and R. L. Webb, Condensation of R-12 in small hydraulic diameter extruded aluminum tubes with and without micro-fins, *Int. J. Heat Mass Transfer* **39,** 791–800 (1996).
2. M. W. Wambsganss, J. A. Jendrzejczyk, D. M. France and N. T. Obot, Two-phase flow patterns and frictional pressure gradients in a small rectangular channel : a comparison between two horizontal orientations, Argonne National Laboratory Report No. ANL-90/46 (1990).
3. M. W. Wambsganss, J. A. Jendrzejczyk and D. M. France, Two-phase flow and pressure drop in flow passages of compact heat exchangers, SAE Technical Paper Series, no. 920550 (1992).
4. C. A. Damianides, Horizontal two-phase flow of air–water mixtures in small diameter tubes and compact heat exchangers, Ph.D. Dissertation, University of Illinois at Urbana-Champaign, Urbana, IL (1987).
5. P. Thors and J. E. Bogart, In-tube evaporation of HCFC-22 with enhanced tubes, *J. Enhanced Heat Transfer* **1** (4), 365–378 (1994).
6. L. M. Chamra, R. L. Webb and M. R. Randlett, Advanced micro-fin tubes for condensation, *Int. J. Heat Mass Transfer* (in press).
7. W. M. Kays and A. L. London, *Compact Heat Exchangers* (3rd Edn), pp. 108–114. McGraw-Hill, New York (1984).
8. J. G. Collier and J. R. Thome, *Convective Boiling and Condensation* (3rd Edn), pp. 53, 54, 106–112. Oxford University Press, Oxford, U.K. (1994).
9. S. M. Zivi, Estimation of steady state steam void-fraction by means of principle of minimum entropy production, *Trans. ASME, Ser. C* **86,** 237–252 (1964).
10. W. W. Akers, H. A. Deans and O. K. Crosser, Condensation heat transfer within horizontal tubes, *Chem. Engng Prog. Symp. Ser.* **55**(29), 171–176 (1959).
11. T. C. Carnavos, Heat transfer performance of internally finned tubes in turbulent flow, *Heat Transfer Engng* **4**(1), 32–37 (1980).
12. R. L. Webb, *Principles of Enhanced Heat Transfer*, p. 209. Wiley Interscience, New York (1994).
13. R. W. Lockhart and R. C. Martinelli, Proposed correlation of data for isothermal two-phase, two-component flow in pipe, *Chem. Engng Prog. Symp. Ser.* **45**(1), 39–48 (1949).
14. D. Chisholm, A theoretical basis for the Lockhart–Martinelli correlation for two-phase flow, *Int. J. Heat Mass Transfer* **10,** 1768–1778 (1967).
15. M. W. Wambsganss, J. A. Jendrzejczyk, D. M. France and N. T. Obot, Frictional pressure gradients in two-phase flow in a small horizontal rectangular channel, *Exp. Thermal Fluid Sci.* **5,** 40–56 (1992).
16. R. C. Martinelli and D. B. Nelson, Prediction of pressure drop during forced-circulation boiling of water, *Trans. ASME* **70,** 695–702 (1948).